

Article

Microstructure and Mechanical Properties of Ultrasonic Welded Joint of 1060 Aluminum Alloy and T2 Pure Copper

Guanpeng Liu, Xiaowu Hu, Yanshu Fu and Yulong Li *

Key Lab of Robot & Welding Automation of Jiangxi Province, Mechanical & Electrical Engineering School, Nanchang University, Nanchang 330031, China; guanpengliu@email.ncu.edu.cn (G.L.); huxiaowu@ncu.edu.cn (X.H.); yshfu@ncu.edu.cn (Y.F.)

* Correspondence: liyulong@ncu.edu.cn; Tel.: +86-0791-8396-9630

Received: 20 July 2017; Accepted: 7 September 2017; Published: 11 September 2017

Abstract: The microstructure and mechanical properties of Al/Cu ultrasonic welding joints were investigated. Results show that: (i) the joint strength increased when the welding time increased within a certain range, and a maximal resistant force of 163.04 N was obtained when the welding duration and welding static pressure were 200 ms and 7.2 MPa, respectively; (ii) with a further increase of welding time, the bonding interface was gradually occupied by a thick strip layer of brittle Al_2Cu (θ_2) phase, thus decreasing the strength; (iii) the maximum temperature in the welding region was 360 °C during the welding process, and a recrystallization phenomenon was identified near the welding interface; (iv) the average nanohardness of Cu, the Cu-Al interfacial reaction layer and Al were 1.04 GPa, 1.34 GPa, and 0.53 GPa, respectively, which is consistent with the formation of the intermetallic compound identified by energy-dispersive X-ray spectroscopy (EDS) and XRD analysis.

Keywords: ultrasonic welding; aluminum; copper; microstructure; mechanical property; nanoindentation

1. Introduction

The ultrasonic welding process utilizes ultrasonic energy and pressure to induce an oscillating shear strain between the faying surfaces and produce a metallurgical bond. An ultrasonic welding process takes some milliseconds, with hardly changing properties of the welding samples. Ultrasonic welding is low cost and has a short welding cycle compared with electrical resistance spot welding [1] and friction stir welding [2]; ultrasonic welding also has the advantage of small distortion or shrinkage [3] compared to fusion welding [4]. With the development of high-power ultrasonic equipment, ultrasonic welding has been widely used in the industry of electron, electricity, packaging, aerospace, and nuclear energy due to its merits.

Copper and aluminum alloys are among the most widely used nonferrous metals in industry. Furthermore, the Cu/Al dissimilar metal joints are extensively applied in the electricity, packaging, ground, and space vehicles industry due to desired thermal and electrical conductivity [5]. Lee et al. [6] have researched the electrical and mechanical properties of friction welded Cu/Al bimetal joints. Asemabadi et al. [7] have investigated the mechanical properties of explosive-welded Cu/Al bimetal. Avettand-Fenoel et al. [8] have studied interfacial intermetallic compound (IMC) in a friction-stir welded Cu/Al. However, detrimental hard and brittle IMC can easily form at the interface in the fusion welding and brazing process. Additionally, significant surface preparations are required for a successful brazing process of aluminum and copper because of the surface oxides [9]. An ultrasonic welding process, performed by a simple facility, allows for an easy joining in a short time without significant surface preparations, owing to the local frequent friction and extreme deformation experienced at the interface.

Although the ultrasonic welding of aluminum and copper alloy has been conducted previously [10,11], the mechanism of bonding formation and reaction phases of the joint are not well understood due to the small weld's size and short welding duration. Additionally, the maximum temperature in the welding region, the mechanical properties of the joint strength, the microstructure characters, and the defects should be studied in detail. As a tool to explore the mechanical properties and microstructural features of small-scale or small-volume samples, nanoindentation is becoming popular in material research and has been successfully used to probe the small-scale mechanical properties of many materials [12]. In this paper, copper and aluminum sheets were welded using the ultrasonic spot welding method. The following topics were discussed to further understand the microstructural evolution and formation mechanism of the welded joint in detail: (i) the joint strength in terms of resistant force to the tensile, welding parameters and microstructure characteristics of the joint; (ii) the effects of the surface preparations on the joint strength; (iii) the temperature rise in the welding region during the ultrasonic welding process; (iv) the nanohardness of the Cu-Al interfacial reaction layer.

2. Materials and Experimental Procedures

The ultrasonic welding was performed using the 1060 aluminum alloy and T2 copper sheets with the same thickness of 0.5 mm; during welding, the copper was put on the top of the aluminum. The welded spot with a size of 5 mm × 5 mm was located at the centre of 25 mm overlap on 100 mm × 20 mm strips, as shown in Figure 1. The welding equipment used in this research work is an ultrasonic spot welding machine (Nicle ultrasonic equipment Co., Ltd., Wuxi, China) with the output power of 0~4500 W, a vibration amplitude of 35 μm, a vibration frequency of 20 kHz, and the welding static pressure of 5.4~9.0 MPa. The sonotrode and anvil, each of which has a serrated working surface, are made of high-speed steel.

In order to determine the optimum welding conditions, a full factorial design was used in the experiments. The major parameters of the ultrasonic welding process are the static pressure and welding duration. In this study, three static pressures, i.e., 5.4, 7.2, and 9.0 MPa were selected and generated by the welding equipment, and the welding durations were set as 60, 80, 100, 120, 140, 160, 180, 200, 220, 240, 260 and 280 ms. The post-welding mechanical properties of the joints were tested by tensile lap shear tests using an Instron-1186 tensile testing machine (Instron China Co., Ltd., Shanghai, China) with a crosshead speed of 1 mm/min. The average strength of the joints was determined with five joints produced under the same conditions. Selected joints were cross-sectioned at the center plane that is perpendicular to the welding direction for an optical metallographic analysis. The interfaces and microstructures of the joints were analyzed using a scanning electron microscopy (SEM, FEI, Hillsboro, OR, USA) equipped with an energy-dispersive X-ray spectroscopy (EDS) detector. Thermal cycles during welding were measured using the 0.05 mm diameter k-type microthermocouples that were closely welded to the center of welded spot, as shown in Figure 1. In addition, an iMicro nanoindenter (Nanomechanics, Inc., Oak Ridge, TN, USA) with the load resolution of 6 nN and the displacement resolution of 0.04 nm were used to measure the mechanical properties of the IMC. In this experiment, the continuous measurement of contact stiffness technology (CSM) [13] and the Oliver–Pharr method [14] were used to measure the evolutions of the hardness and Young's modulus with the depth of indentation.

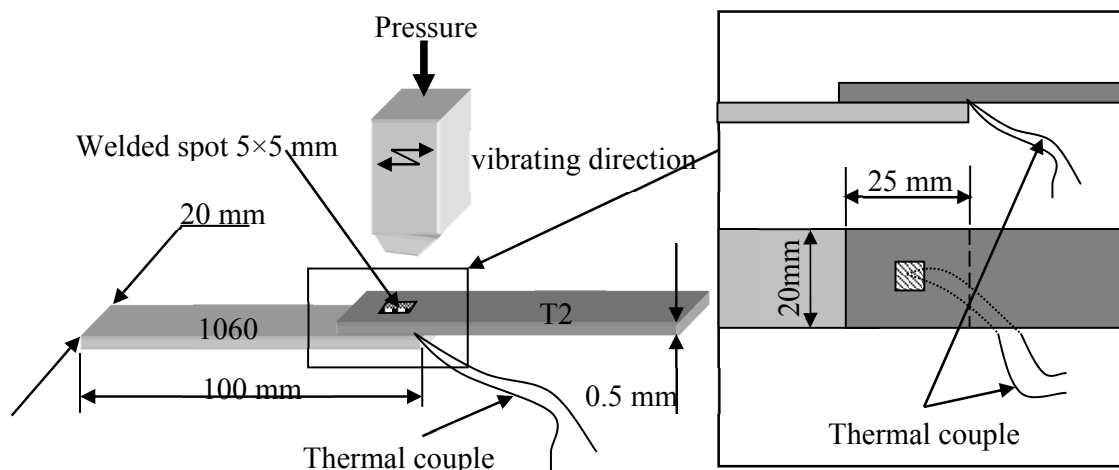


Figure 1. The sketch of a welded specimen.

3. Results and Discussions

3.1. Tensile Shear Test

Figure 2 illustrates the tensile shear test results, i.e., the resistance forces to tensile vs. welding duration and static pressure. It is shown that the tensile resistance tends to increase gradually as the welding time increases under certain static pressures, i.e., 5.4, 7.2, and 9.0 MPa, and as the welding duration increases, the tensile resistance reaches a maximum value, and then decreases. It also can be noticed that when the welding duration was 200 ms and the static pressure is 7.2 MPa, the optimal joint with the strength of 163.04 N was obtained.

A lower resistance force of a joint with a short welding time may be attributed to the defects in the joint: during the welding process, a joint with some micro-regions where no atomic bonds are present is produced due to a short welding time and/or the presence of residue oxides and/or oils at the interface. When the welding time reaches a certain value, above which the friction between and the oscillation of the mating surfaces are sufficient, the associated deformation is satisfactory with no obvious defects, thus forming a joint with a maximum strength. However, with a further extension of the welding duration over a certain value, the joint strength rapidly decreased. The reasons for the strength decrease can presumably be ascribed to the following: (i) the plastic zone (heat-affected zone) can expand rapidly due to the long welding duration inducing over-friction between the mating surfaces, which may weaken the joint properties; (ii) after being subjected to a high temperature with an excessive welding duration, microfatigues or even macrocracks may be induced near the joint zone, thus reducing the welding strength dramatically; (iii) the higher local temperatures and strain rate promote chemical reaction and accelerate diffusion, the thickness of the brittle IMC layer increases, and the lap shear strength decreases. The experimental results above are consistent with previous studies that join similar and dissimilar metals using ultrasonic welding [15].

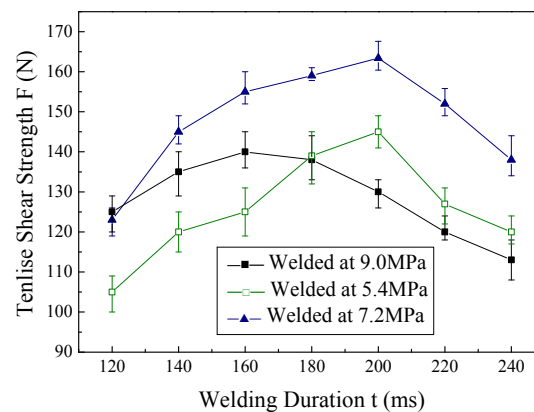


Figure 2. The tensile shear test results: strength vs. welding duration and static pressure.

3.2. Microstructure Characteristics and Their Effects on the Strength

Figure 3 shows the microstructure of the joints welded with different welding durations under a static pressure of 7.2 MPa. As shown in Figure 3a–d, each welded joint has a satisfactory welding interface without hollow pores nor exfoliation; the formation of IMC at the interface can be visually confirmed in Figure 3b–d. Furthermore, it seems that the width of the reaction layer increases as the welding time is prolonged. High local temperatures and strain rate and pressure promote chemical reaction and accelerate diffusion, which leads to metallic bonding between the two sheets [16]. When the welding time is 120 ms, the reaction layer is too thin to be seen, or there is no reaction layer at all; when the welding time is 160 ms, the width of the reaction layer is about 1~2 μm ; when the welding time is 200 ms, the width of the reaction layer is about 3~4 μm ; when the welding time is 240 ms, the reaction layer is about 3~5 μm . One reason is that as the welding time increases, the welding energy increases; so, the atoms diffusion and reaction rate increases accordingly. Another reason is that the temperature of the interface significantly increases with the welding durations, which results in an exponential increase of the atomic diffusion coefficient [17].

EDS analysis results show that the reaction layer at the interface of the welded joint is mainly composed of Al and Cu, with the proportion of about 2:1 (confirmed by three tested points of the reaction layer of each specimen). This layer may be Al_2Cu phase layer, according to the Al-Cu binary phase diagram [18]. In addition, although there seems to be no reaction layer at the interface of the joint welded with the 120 ms duration, the EDS line scan shows an obvious interdiffusion between Al and the Cu base metal, as shown in Figure 4. It should be pointed out that the width of the reaction layer and the joint strength can be well correlated (as shown in Figures 2 and 3): when the welding time is short, the strength of the joint is not high due to insufficient diffusion between the metals. With an increase of the welding duration increasing energy input, the lap shear strength was increased in the beginning, owing to high temperatures and strain rate, which accelerate diffusion between the Cu and Al alloy. When the welding time is further increased, the Al/Cu interface is gradually occupied by a thick strip layer of brittle Al_2Cu (θ_2) phase, thus decreasing the strength. Figure 5 presents the typical fracture path and XRD patterns of the Al/Cu joint welded at 240 ms, and the formation of the continuous Al_2Cu phase layer can cause the low strength, although it strengthens a few fractions of the joint zone. When the welding duration is further increased, a great quantity of brittle phases at a local place may decrease the joint strength dramatically, and the severe deformation-induced cracks may destroy the joint, as shown in Figure 6. Intermetallic formation is commonly assumed to be deleterious to mechanical properties and undesired in the cases of Al/Cu diffusion bonding [19]. Therefore, a control of intermetallic formation should be further investigated.

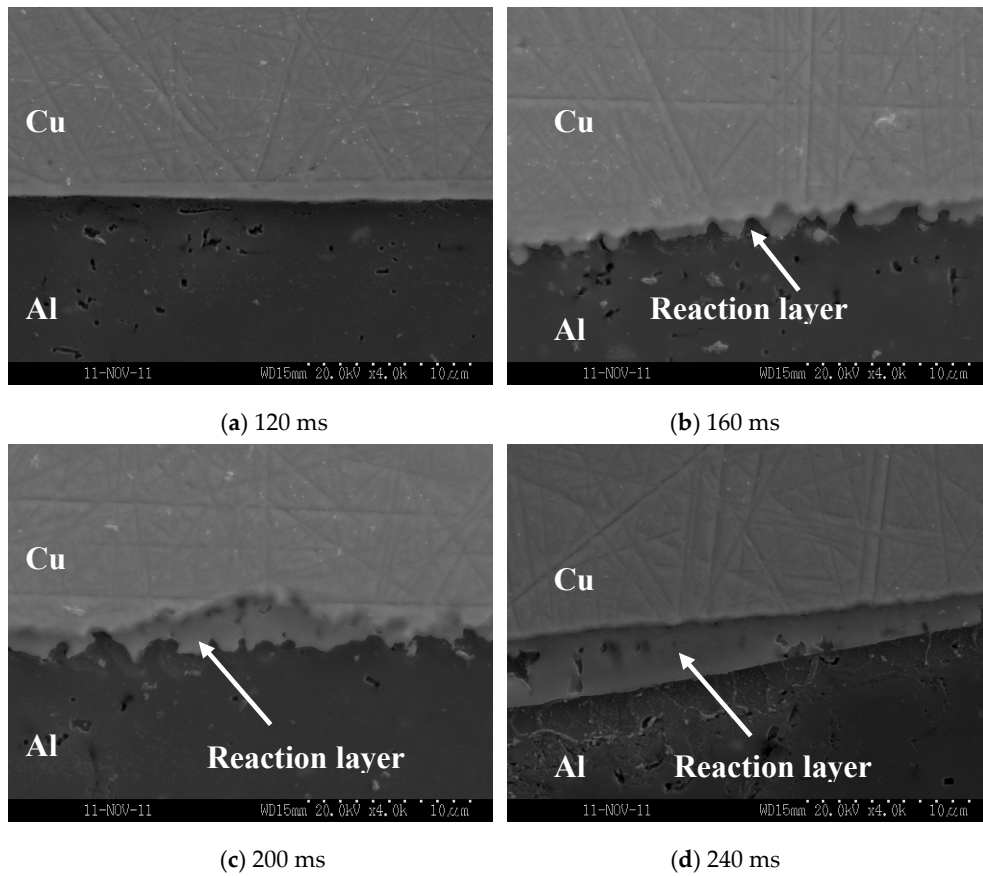


Figure 3. Scanning electron microscopy (SEM) images of the cross-section of the joints welded with different welding duration, which show a growth trend of the reaction layer.

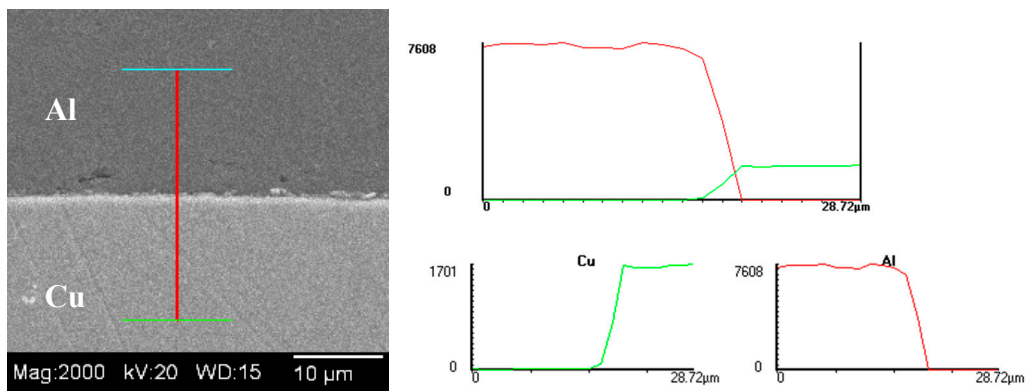


Figure 4. Energy-dispersive X-ray spectroscopy (EDS) line scan across the interface of the Al/Cu joint: showing an obvious interdiffusion of the Al and Cu.

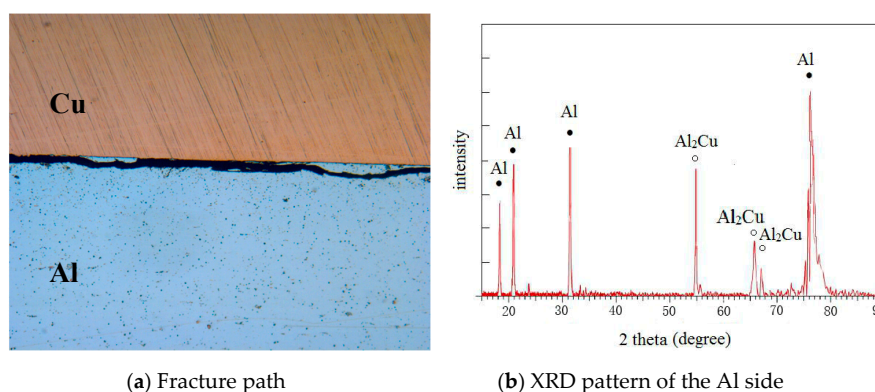


Figure 5. Fracture path and XRD pattern of the fracture surface of the joint welded with the 240 ms duration.

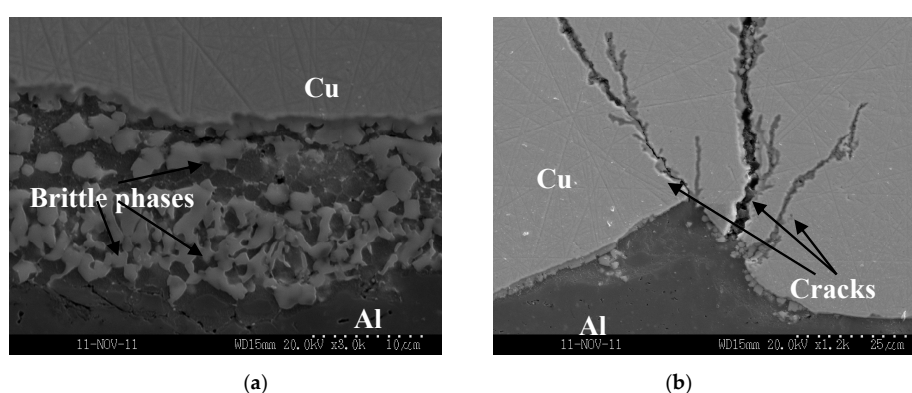


Figure 6. (a) Brittle phases and (b) Cracks defect of the Al/Cu ultrasonic welded joint.

Generally speaking, surface characteristics, including surface finish, oxides, coatings, and contaminants on a base metal, are of significant importance to welding or brazing process [20,21]. However, it is not easy to quantitatively study the effects of the surface characteristics during ultrasonic welding. As surface characteristics can be changed by the preparations, i.e., surface cleaning, the effects of the surface characteristics on the ultrasonic welding of aluminum and copper were studied using two groups of samples of different surface cleaning: one group of samples were sequentially cleaned by the dilute acid, alkali solution, and acetone for removing the oxides and contaminants on the surfaces; the other group was used as the given state without any preparation. The static pressure was set as 7.2 MPa, and the welding duration was set as 90, 130, 150, 210 and 230 ms. At each welding condition, five Al/Cu welded joints were acquired for a tensile shear test. Table 1 shows the comparison of the joint strength with and without surface cleaning. Results show that surface preparations have little effect on the aluminum alloy and pure copper ultrasonic welding process. In other words, a trace amount of oxides or oils do not affect the joint properties. The reason is that the metal sheets were held on the sonotrode prior to welding; when the pressure and ultrasonic vibration were applied to the sonotrode, friction and deformation were experienced at the interface between the metal sheets. As a result, the oxides or oils were damaged and extruded out of welding zone, thus, a bond formed between the fresh surfaces under the friction and pressure.

Table 1. Effects of surface preparations on the joint strength.

Welding Duration	90 ms	130 ms	150 ms	210 ms	230 ms
Cleaned	95.328 N	102.123 N	127.633 N	156.56 N	136.337 N
Uncleaned	97.605 N	100.503 N	123.609 N	150.24 N	138.257 N

3.3. Temperature in the Welded Zone

During the ultrasonic welding process, friction between the surfaces, vibration, and deformation of the base metals induced temperature rise in the welding zone [22]. Measuring the temperature rise in the weld area is important for identifying the heat affected zone (HAZ) as well as the quantity of temperature generated and an understanding of the mechanism of the process [23].

In order to estimate the experimental temperature rise around the joint interface, a pair of thermocouples with the diameter of 0.05 mm was spot welded in the middle of welding zone, as shown in Figure 1. The data of the welding temperature vs. the welding duration with the static pressure of 7.2 MPa, as depicted in Figure 7, show an increasing trend of temperature rise over the welding time. When the welding duration was 0.28 s, the welding temperature was up to 350 °C, and the recrystallization phenomenon was found near the interface, as shown in Figure 7b. However, the welded specimen adhibited to the welding sonotrode when the welding time was longer than 0.26 s (i.e., 0.28 s) due to a high temperature in the welding zone, the deformation, and the friction. Therefore, the welding duration cannot be increased further in the conditions used in this paper. The previous studies of the temperature rise during the ultrasonic welding presented the similar results. D. Bakavos et al. [4] measured the temperature rise of an ultrasonic spot bonding of aluminum, and pointed out that the temperature rose extremely quickly and the temperature was affected by the ultrasonic energy. In addition, in order to get a perfect joint, the ultrasonic energy (or welding duration) should not be too high, because that the temperature rise may induce a strength loss of the metals [24].

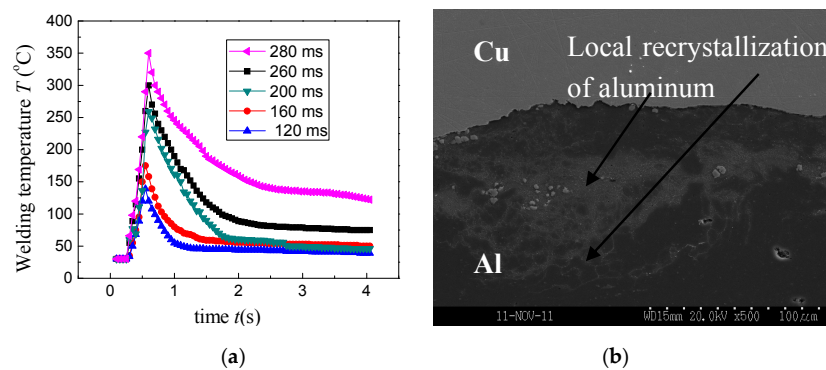


Figure 7. (a) Welding temperatures vs. welding durations, static pressure 7.2 MPa (b) Local recrystallization of aluminum.

3.4. Nanoindentation Test Analysis

As mentioned above, the precise hardness values of the IMC are difficult to obtain by the general microscopic hardness measurement due to the small thickness of the reaction layer (1–10 μm). As shown in Figure 8, in order to obtain a reliable hardness value of the reaction layer, the nanoindenter with 2000 nm indentation depth and 3×3 matrix point mode was adopted.

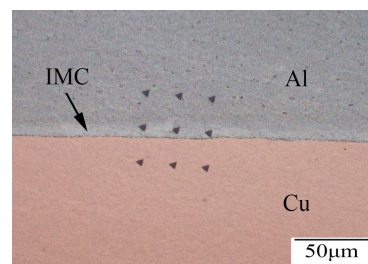


Figure 8. Nanoindentation test on the interface of the joint welded with the 240 ms duration under the static pressure of 7.2 MPa.

Figure 9a shows the load-displacement curves of the different regions. It is noted that a load-displacement curve is mainly composed of three parts: (i) in the loading stage, the elastic deformation occurs when the indenter touches the specimen; with the deepening of the indentation depth, the elastic deformation gradually transforms into plastic deformation, and then the plastic deformation increases continuously; (ii) in the continuous loading stage, when the load reaches the maximum, it remains constant for 10 s; as we can see a small straight line on the curve, the load remains constant, but the depth of penetration increased continuously, and the creep deformation occurs in the specimen; (iii) in the unloading stage, the indenter is unloaded until the load is zero, which results in a residual indentation depth due to the presence of plastic deformation. As the 3×3 matrix point mode was adopted, the maximum load reaches the same depth in the three different tested points of the same phase. It can be noted that in order to get the same depths, the IMC demands the largest load, followed by Cu and Al due to the hardness differences, as can be seen in Figure 9b.

Figure 9b,c is the hardness-displacement curve and Young's modulus-displacement curve at the interface based on the contact stiffness continuous measurement technology (CSM) [13]. As shown in Figure 9b, the hardness is observed to decrease with the increasing depth of indentation within a certain range, then, it gradually smooths. In addition, the hardness of the points in each region of the reaction layer has little discrepancies, which indicate that the reaction layer is not homogeneous, so the hardness value changes a little. According to Figure 9c, although there are some small fluctuations in the curves, they generally shows a similar trend. In general, the curves show that the values obtained by nanoindentation are reliable.

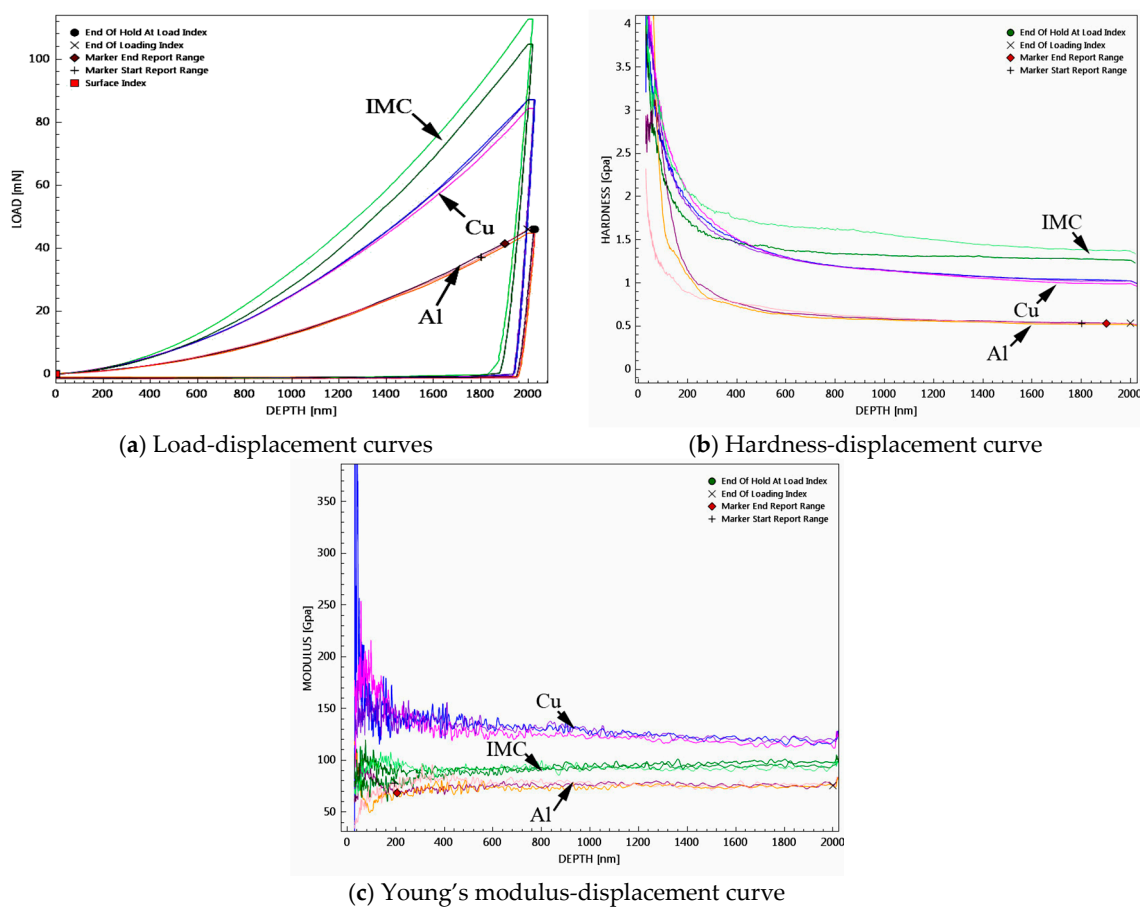


Figure 9. Result of nanoindentation test.

Figure 10 shows that the Young's modulus of the Al, the Cu, and the Cu-Al reaction layer are 75.5 GPa, 118.4 GPa and 95.3 GPa, respectively, and the average hardness of the Al, the interfacial

reaction, and the Cu were 0.53 GPa, 1.34 GPa, and 1.04 GPa, respectively. The high hardness of the reaction layer indicates that this region produced the hard and brittle IMC. Through the EDS and XRD, it is conformed to be Al_2Cu . It is well known that in dissimilar joints, the presence of the IMC is an indication of a sound weld. A thin, continuous and uniform IMC layer is necessary for sound joints [25]. However, the thickness of the reaction layer increases with the increase of welding energy, which may result in a large number of hard brittle IMC at the interface, and deteriorate the mechanical properties of the joints due to the properties of IMC [25]. It was reported that if the total thickness of the IMC layer is less than 2 μm , the Cu-Al joints maintained their mechanical properties [26]. Therefore, optimizing the welding parameters such as the welding time and welding pressure to control the welding energy, and then reduce the generation of the IMCs, is indispensable.

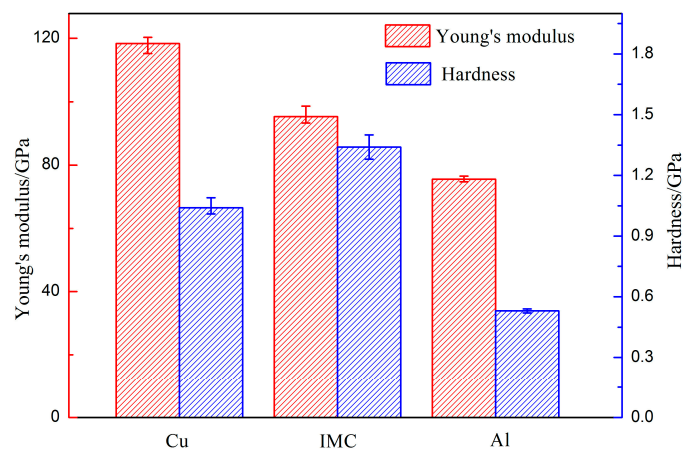


Figure 10. Average nanohardness and Young's modulus of each tested point.

4. Conclusions

1060 aluminum alloy and T2 copper sheets were bonded by using ultrasonic welding method. Joint strength, microstructure characteristics of the joint, effects of the surface preparations on the joint strength, and temperature rise in the welding region were studied.

According to the experimental results and theoretical analysis, several conclusions can be drawn as follows: (i) owing to the combined strengthening effects of the interdiffusion between the aluminum and copper base metals, the joint strength increased when the welding time increased within a certain range, and a maximal resistant force of 163.04 N was obtained when the welding duration was 200 ms and the welding static pressure was 7.2 MPa; with a further increased welding time, the bonding interface was gradually occupied by a thick strip layer of brittle Al_2Cu (θ_2) phase. The hardness of the IMC when the welding duration was 240 ms and welding static pressure was 7.2 MPa was relatively higher (1.34 GPa) than the aluminum (0.53 GPa) and Copper (1.04 GPa), thus decreasing the strength; when the welding time was longer than 280 ms, the joint strength was poor due to the formation of the thick brittle Al_2Cu layer and the mutual adhesion between the sample and the sonotrode; (ii) surface preparations had little effect on the aluminum and copper ultrasonic welding process and resulted joint strength under the conditions considered in this paper; (iii) maximum temperature in the welding region was 360 °C during the welding, and a recrystallization phenomenon was identified near the interface.

Acknowledgments: The research was sponsored by the National Natural Science Foundation of China (No.51665039) and the Key research and development project of Jiangxi Province (20171BBE50009).

Author Contributions: Yulong Li and Guanpeng Liu conceived and designed the experiments; Guanpeng Liu performed the experiments; Yulong Li and Xiaowu Hu analyzed the data; Yanshu Fu contributed sample fabrication; Guanpeng Liu wrote the paper. All authors contributed to the data analysis and discussion.

Conflicts of Interest: The authors declare no conflict of interest.

References

1. Peng, J.; Fukumoto, S.; Brown, L.; Zhou, N. Image analysis of electrode degradation in resistance spot welding of aluminium. *Sci. Technol. Weld. Join.* **2004**, *9*, 331–336. [[CrossRef](#)]
2. Brassington, W.D.P.; Colegrove, P.A. Alternative friction stir welding technology for titanium-6Al-4V propellant tanks within the space industry. *Sci. Technol. Weld. Join.* **2017**, *22*, 300–318. [[CrossRef](#)]
3. Bakavos, D.; Prangnell, P.B. Mechanisms of joint and microstructure formation in high power ultrasonic spot welding 6111 aluminium automotive sheet. *Mater. Sci. Eng. A* **2010**, *527*, 6320–6334. [[CrossRef](#)]
4. Feng, M.; Li, Y.; Zhao, C.; Luo, Z. Mechanical properties and interface morphology of Mg/Al ultrasonic spot weld bonding welds. *Sci. Technol. Weld. Join.* **2016**, *21*, 688–699. [[CrossRef](#)]
5. Celik, S.; Cakir, R. Effect of friction stir welding parameters on the mechanical and microstructure properties of the Al-Cu butt joint. *Metals* **2016**, *6*, 133. [[CrossRef](#)]
6. Lee, W.B.; Bang, K.S.; Jung, S.B. Effects of intermetallic compound on the electrical and mechanical properties of friction welded Cu/Al bimetallic joints during annealing. *J. Alloys Compd.* **2005**, *390*, 212–219. [[CrossRef](#)]
7. Asemabadi, M.; Sedighi, M.; Honarpisheh, M. Investigation of cold rolling influence on the mechanical properties of explosive-welded Al/Cu bimetal. *Mater. Sci. Eng. A* **2012**, *558*, 144–149. [[CrossRef](#)]
8. Avettand-Fenoel, M.N.; Taillard, R.; Ji, G.; Goran, D. Multiscale Study of Interfacial Intermetallic Compounds in a Dissimilar Al 6082-T6/Cu Friction-Stir Weld. *Metall. Mater. Trans.* **2012**, *43*, 4655–4666. [[CrossRef](#)]
9. Xia, C.; Li, Y.; Puchkov, U.A.; Gerasimov, S.A.; Wang, J. Microstructure and phase constitution near the interface of Cu/Al vacuum brazing using Al-Si filler metal. *Vacuum* **2008**, *82*, 799–804. [[CrossRef](#)]
10. Matsuoka, S.I.; Imai, H. Direct welding of different metals used ultrasonic vibration. *J. Mater. Process. Technol.* **2009**, *209*, 954–960. [[CrossRef](#)]
11. Satpathy, M.P.; Sahoo, S.K. Microstructural and mechanical performance of ultrasonic spot welded Al-Cu joints for various surface conditions. *J. Manuf. Process.* **2016**, *22*, 108–114. [[CrossRef](#)]
12. Meng, Y.; Wang, S.; Cai, Z.; Young, T.M.; Du, G.; Li, Y. A novel sample preparation method to avoid influence of embedding medium during nano-indentation. *Appl. Phys. A Mater. Sci. Process.* **2013**, *110*, 361–369. [[CrossRef](#)]
13. Pharr, G.M.; Oliver, W.C.; Brotzen, F.R. On the generality of the relationship among contact stiffness, contact area, and elastic modulus during indentation. *J. Mater. Res.* **1992**, *7*, 613–617. [[CrossRef](#)]
14. Oliver, W.C.; Pharr, G.M. An improved technique for determining hardness and elastic modulus using load and displacement sensing indentation experiment. *J. Mater. Res.* **1992**, *7*, 1564–1583. [[CrossRef](#)]
15. Panteli, A.; Robson, J.D.; Brough, I.; Prangnell, P.B. The effect of high strain rate deformation on intermetallic reaction during ultrasonic welding aluminium to magnesium. *Mater. Sci. Eng. A* **2012**, *556*, 31–42. [[CrossRef](#)]
16. Haddadi, F. Rapid intermetallic growth under high strain rate deformation during high power ultrasonic spot welding of aluminium to steel. *Mater. Des.* **2015**, *66*, 459–472. [[CrossRef](#)]
17. Wert, C.; Zener, C. Interstitial Atomic Diffusion Coefficients. *Phys. Rev.* **1949**, *76*, 1169–1175. [[CrossRef](#)]
18. Yan, X.Y.; Chang, Y.A.; Xie, F.Y.; Zhang, F.; Daniel, S. Calculated phase diagrams of aluminum alloys from binary Al-Cu to multicomponent commercial alloys. *J. Alloys Compd.* **2001**, *320*, 151–160. [[CrossRef](#)]
19. Guo, Y.; Liu, G.; Jin, H.; Shi, Z.; Qiao, G. Intermetallic phase formation in diffusion-bonded Cu/Al laminates. *J. Mater. Sci.* **2011**, *46*, 2467–2473. [[CrossRef](#)]
20. AlShaer, A.W.; Li, L.; Mistry, A. The effects of short pulse laser surface cleaning on porosity formation and reduction in laser welding of aluminium alloy for automotive component manufacture. *Opt. Laser Technol.* **2014**, *64*, 162–171. [[CrossRef](#)]
21. Liu, L.; Zhou, S.Q.; Tian, Y.H.; Feng, J.C.; Jung, J.P.; Zhou, Y.N. Effects of surface conditions on resistance spot welding of Mg alloy AZ31. *Sci. Technol. Weld. Join.* **2009**, *14*, 356–361. [[CrossRef](#)]
22. Chang, U.I.; Frisch, J. On Optimization of Some Parameters in Ultrasonic Metal Welding. *Weld. J.* **1974**, *53*, 24–35.
23. De Vries, E. Mechanics and Mechanism of Ultrasonic Metal Welding. Ph.D. Dissertation, The Ohio State University, Columbus, OH, USA, 2004.
24. Hongoh, M.; Miura, H.; Ueoka, T.; Tsujino, J. Temperature Rise and Welding Characteristics of Various-Frequency Ultrasonic Plastic Welding Systems. *Jpn. J. Appl. Phys.* **2006**, *45*, 4806–4811. [[CrossRef](#)]

25. Laurila, T.; Vuorinen, V.; Kivilahti, J.K. Interfacial reactions between lead-free solders and common base materials. *Mater. Sci. Eng. R* **2005**, *49*, 1–60. [[CrossRef](#)]
26. Braunovic, M.; Aleksandrov, N. Intermetallic compounds at aluminum-to-copper and copper-to-tin electrical interfaces. In Proceedings of the 38th IEEE Holm Conference on Electrical Contacts, Philadelphia, PA, USA, 18–21 October 1992; pp. 25–34.



© 2017 by the authors. Licensee MDPI, Basel, Switzerland. This article is an open access article distributed under the terms and conditions of the Creative Commons Attribution (CC BY) license (<http://creativecommons.org/licenses/by/4.0/>).